Aircraft Measurement of Mesoscale Pressure Gradients and Ageostrophic Winds

ALFRED R. RODI AND THOMAS R. PARISH

Department of Atmospheric Science, University of Wyoming, Laramie, Wyoming

(Manuscript received 9 February 1987, in final form 17 July 1987)

ABSTRACT

Determination of the horizontal pressure gradient force over distance scales less than 100 km is possible using airborne altimetry and detailed maps of the underlying terrain. To detect the very small isobaric slopes, instrumentation must perform up to specification and aircraft position must be known within about 250 m in order to achieve an adequate matching of altimeter height and terrain height. Numerous test flights were conducted to study the stability of the technique. Results indicate the system is capable of resolving pressure gradients with equivalent geostrophic wind errors of approximately ±1 m s^{-1} over a 100 km horizontal scale.

1. Introduction

Geostrophy is a widely accepted construct for large-scale atmospheric motions. Scale analysis of the horizontal equations of motion (i.e., Holton, 1979) and case studies (Shapiro, 1970, for example) clearly suggest the pressure gradient and Coriolis forces are the largest terms for large-scale midlatitude upper-level tropospheric motions. Although the quasi-geostrophic view of synoptic scale motions provides a relatively simple and qualitatively correct picture of large-scale dynamics, recent studies have recognized the importance of the ageostrophic components and have focused on the imbalances of the dynamic processes at work. Uccellini and Johnson (1979) have shown that the ageostrophic motions associated with the mass and momentum adjustments in a propagating jet streak contribute significantly to the development of a low-level jet beneath the exit region. Uccellini et al. (1984) among others note that the magnitude of such ageostrophic components can comprise a significant fraction of the entire wind under certain conditions and contribute to significant weather events. Ageostrophic winds in excess of 30 m s^{-1} were inferred by the above authors for the Presidents' Day cyclone of 18–19 February 1979, and a clear association between ageostrophic nature of the lower atmosphere and development of heavy snow were noted.

In general, accurate detection of ageostrophic winds is difficult. Uccellini et al. (1984) showed that a consistent picture of the ageostrophic circulations associated with upper-level jet streaks is obtainable using rawinsonde data provided some care is taken to ensure internal consistency of the dataset. However, even slight errors in either analysis or measurement seriously degrade the fidelity of rawinsonde-derived ageostrophic winds. Shapiro and Kennedy (1981) note that small, uncorrelated temperature errors lead to serious errors in upper-level geostrophic winds. Small directional errors (<10°) and/or uncertainties in the orientation of the horizontal pressure gradient force also contribute to significant errors in the ageostrophic wind determination since the angle between the wind and the height contours is almost always less than 30°. In addition, the coarse spatial and temporal resolution (400 km and 12 h) of rawinsonde data precludes detailed study of most subsynoptic phenomena. The purpose of this paper is to report on an in situ measurement technique using radar altimetry onboard an instrumented aircraft to measure the geostrophic wind directly over distance scales of 100 km or less. Using concurrent wind measurement derived from inertial navigation system (INS) and gust probe data on the aircraft, the mesoscale ageostrophic components can be obtained.

During July 1983 and again in May 1985 and March–April 1986, field programs were conducted in northcentral Oklahoma to study the ageostrophic motions and resulting accelerations responsible for the diurnal evolution of the Great Plains low-level jet (LLJ). The primary database was obtained using an instrumented research aircraft as the observational platform. Stimulus for the experiments came from the realization that precise and high resolution radar altimeters and inertial navigation systems (INS) on research aircraft had the potential for measuring the slope of isobaric heights over horizontal scales 100 km or less. Bellamy (1945) first suggested the use of radar altimetry for measuring the slope of isobaric surfaces and the use of the "*D*-value," or difference in height between the U.S. Standard Atmosphere pressure altitude and the measured radar altitude (above mean sea

Corresponding author address: Dr. Alfred Rodi, Dept. of Atmospheric Sciences, University of Wyoming, P.O. Box 3038, University Station, Laramie, Wyoming 82071.

level), in the equation of motion. Brown et al. (1981) described the application of modern aircraft instrumentation to D-value measurement. The pioneering work of Shapiro and Kennedy (1981, 1982) used the technique to study midlatitude jet stream dynamics over the ocean and over complex terrain. Shapiro and Kennedy estimated that the errors in D-value computations were ±6 m over ocean and ±10 m over land. These were very acceptable error margins in those studies since jet stream isobaric slopes approach 10^{-3} (see Fig. 3d in Brown et al., 1981; Fig. 5 in Shapiro and Kennedy, 1982). However, for mesoscale events having a characteristic scale length of 100 km or less and wind speeds on the order of 10 m s^{-1}, discerning the slopes of pressure surfaces becomes much more difficult. Furthermore, in the case of the Great Plains LLJ, the terrain slope is generally an order of magnitude greater than corresponding isobaric slopes.

LeMone and Tarleton (1986) demonstrated the use of inertial altitude (as opposed to pressure altitude) calculated from inertial navigation system (INS) accelerometers to determine the perturbation pressure field at the base of cumulus congestus or cumulonimbus clouds. This approach is limited to scales as small as convective-scale perturbations because of the bias in the vertical accelerometer which must be removed by detrending, under the assumption that the pressure and inertial altitudes are equal at the end points of the flight leg. Thus, only small wavelength features (<20 km) can be resolved with the inertial technique and the larger scale isobaric slope is lost.

Here we use radar altimetry for measuring the slope of isobaric surfaces over land, and demonstrate that ±1 m s^{-1} accuracy is possible in the computation of geostrophic wind components over horizontal scales as small as 100 km, and to examine the potential of aircraft measurements of horizontal pressure gradients on these scales over irregular terrain. The motivation for the study was the desire to resolve mesoscale ageostrophic motions by subtracting the resulting geostrophic winds from the actual winds measured by the aircraft.

In a companion paper, Parish et al. (1987) present a case study of the kinematical and dynamical evolution of the summertime Great Plains low-level jet.

2. Aircraft instrumentation

a. Overview

The University of Wyoming's Beechcraft Super King Air research aircraft (K/A) was the observational platform for the Great Plains LLJ project during which this data was collected. A description of the standard K/A instrumentation, signal processing, and aircraft characteristics may be found in Cooper (1978). Key instruments included a Litton model LTN-51 INS for aircraft attitude and ground speed measurements, a Stewart-Warner model APN-159 radar altimeter, and Rosemount model 1201 and 1501 static pressure sensors.

Measurement of isobaric slopes was made as follows. Flights were conducted at constant pressure using the aircraft autopilot to keep the aircraft within ±1 mb of the desired pressure level. By adding the measured geometric altitude from the radar altimeter each second to the terrain height obtained from U.S. Geological Survey 1:24 000 topographic maps digitized on a 0.4 × 0.4 km grid, the height of the isobaric surface above sea level was calculated. The use of D-value to account for deviations of the aircraft from constant pressure (Shapiro and Kennedy, 1981, 1982) was not used. Rather, minor deviations of the aircraft from the true isobaric surface were corrected by means of the hypsometric equation using actual measurements of the virtual temperature T_v along the track. Variation of T_v along the pressure surface typically has small effect on the resulting values of V_g. In the analyses shown here, however, we used the observed trend in T_v along the track to refine the calculation of these deviations further.

b. Sources of error

Three fundamental measurements from the aircraft are required to derive isobaric slope: geometric altitude, static pressure, and horizontal position. A detailed description of the APN-159 radar altimeter is found in Brown et al. (1981) in which the short-term error was reported to be ±0.43 m, largely synchro backlash error. This short-term error results from the imprecision of the gears inside the synchro devices themselves from which the altitude is picked off by means of synchro-digital converters, and under turbulent level flight involving many small up and down corrections, can be considered random error. Under maneuvers such as porpoising (discussed below), the error is more systematic. In the K/A system, the synchro-to-digital conversion resolution error is ±0.07 m. The resulting short-term error valid over leg lengths of 15–20 min is <0.5 m. The long-term drift characteristic of the instrument (1.69 m over 3.5 h) is not considered important in the present application. In fact, the present uncertainty in our knowledge of the terrain is far larger than the radar altimeter error.

Steps were taken to minimize the problems associated with measurement of the static pressure at the aircraft flight level. The Rosemount 1201 variable capacitance pressure transducer contains electronic circuitry designed to compensate for temperature changes. However, Knowlton (1980) noted that this compensation is subject to large transient errors when rapid temperature changes in excess of 1°C min^{-1} are encountered such as during changes in altitude during sounding operations.

To avoid this potential problem, the transducer was installed in an oven controlled at 50°C, well above ambient temperature, with temperature stability of

±0.2°C. A second anticipated problem was the effect of varying dynamic pressure on the aircraft causing the so-called "static defect" which also could be as large as several mb on an aircraft such as the K/A. Flight passes at various airspeeds at a distance of 100 m abreast of the instrumented tower at the NOAA Boulder Atmospheric Observatory were conducted to evaluate the static defect. The estimated short-term uncertainty in the static pressure measurement in this installation is estimated to be 0.25 mb which at 800 mb and 288 K corresponds to a height error of 2.5 m. In the 1985 and 1986 flights, the Rosemount 1501 high accuracy digital pressure transducer was added to the aircraft. The higher resolution of the 1501, 0.01 mb, minimized digitization errors.

The most important errors in isobaric slope determination involve the requirement for an accurate registration between the aircraft measurements and the underlying terrain. This requires accurate information about both the position of the aircraft and the terrain height.

The undamped INS position data has a nominal drift rate of 2 km h^{-1} which is inadequate for the present purpose. Care was taken to ensure INS temperature stability by allowing 45–60 min for alignment so that actual drift rates in this project were less than the nominal value. However, it is shown below that position uncertainties of 1 km can result in geostrophic wind errors of as much as 10 m s^{-1} even on relatively flat terrain so that some other source of position data was required. Relevant also are uncertainties in the knowledge of the terrain height caused by the disturbed state of the underlying ground surface which may not be recorded in the topographic data. The radar altimeter measures the leading edge of the returned pulse of energy which in the case of a heavily forested region might reflect the level of tree top rather than the surveyed surface. Similar problems might result from the presence of numerous tall buildings. Obviously, an underestimate of the actual height of the pressure surface would result from these effects. During the LLJ study, the K/A was mostly over open land. However, at several points along the flight path large buildings and trees may have affected the altitude signal. The deviations of the derived pressure surface height would be a measure of the uncertainty of the terrain.

3. Analysis of errors in measuring pressure gradient

The expression for the geostrophic wind component in the y direction determined by an aircraft flying along a constant pressure surface in the x direction is

$$V_g = \frac{g}{2\Omega \sin\varphi} \frac{\partial Z}{\partial x} \tag{1}$$

where Z is the height of the constant pressure surface above mean sea level and the other symbols have their usual meteorological meanings. Z consists of three components: (i) the height of the aircraft above the terrain, Z_R, measured by the radar altimeter; (ii) the height of the terrain above mean sea level (MSL), Z_T; and (iii) small deviations from the constant pressure surface (~5 m) caused by turbulence and autopilot response, Z_{dev}. This is diagrammed in Fig. 1.

The procedure used for calculating $\partial Z/\partial x$ is to use a standard least-squares fit to the straight line relationship between Z and x (for example, Bevington, 1969). The relationship between Z and x can be written

$$Z = a(x - \bar{x}) + b \tag{2}$$

where x is the location along the track, $\bar{x}$ is the mean distance, b is the average height of the pressure surface, and a is $\partial Z/\partial x$, the desired isobaric slope used in the evaluation of V_g in (1). This form $(x - \bar{x})$ was chosen so that the errors in the slope and intercept are independent. The variance in the estimate of a can be found using the standard relationship

$$\sigma_a^2 = \frac{Ns^2}{N\sum x_i^2 - (\sum x_i)^2} \tag{3}$$

where N is the number of data points in the leg, s is the sample standard deviation in the estimate of Z, expressed as

$$s^2 = \frac{1}{N-2} \sum [Z_i - b - a(x_i - \bar{x})]^2, \tag{4}$$

which is the result of uncertainties in the measurement of Z. As noted by Brown et al. (1981), these are random errors associated with the short-duration (~20 min) legs. Absolute accuracy need not be considered as it is only the gradient $\partial Z/\partial x$ that is important in this analysis.

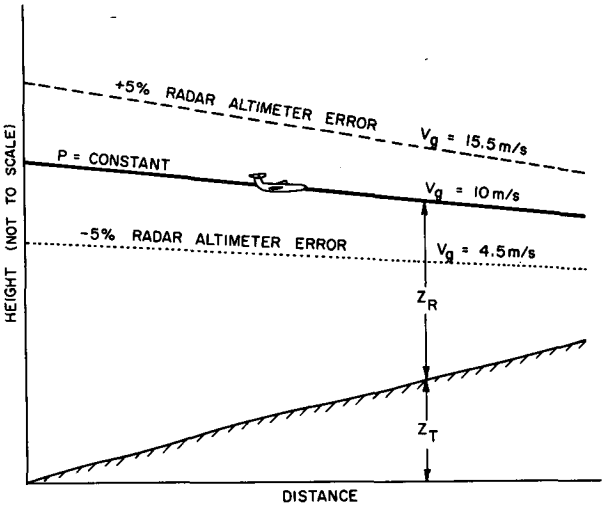

FIG. 1. Description of isobaric slope measurement technique. Terrain slope is assumed to be 10^{-3} and is shown exaggerated 1000×. Terrain slope is exaggerated 250×. Errors in geostrophic wind computation arising from 5% scale error in the radar altimeter are shown (see text). Z_R is the radar altitude and Z_T the terrain height above sea level. Small deviations, Z_{dev}, from constant pressure surface are not shown.

A rough estimate of the error in V_g can be made by evaluating (3) assuming constant groundspeed U and substituting into (1). The denominator of (3) can be estimated by using formulas for the sums of powers of integers ($\sum^N i = N(N+1)/2$, etc.), and assuming $N \gg 1$, as

$$\sigma_a^2 = \frac{12s^2}{\Delta_x^2 N^3} \tag{5}$$

where

$$\Delta_x = U\Delta t$$

$$N = \frac{L}{\Delta_x}$$

$$s^2 = \sigma_{T,1}^2 \tag{6}$$

where N observations at intervals of Δt are taken at ground speed U, L is the total leg length, and $\sigma_{T,1}^2$ is the error in the terrain determination for 1-sec (100 m) data. Substituting into (5) yields an estimate of the error in a, the isobaric slope

$$\sigma_a^2 = \frac{12\sigma_{T,1}^2 U}{L^3}. \tag{7}$$

Substituting (7) into (1) results in an expression for the estimate of the rms error in V_g as

$$\sigma_{V_g}^2 = \frac{g}{2\Omega \sin\varphi}\left[\frac{12\sigma_{T,1}^2 U}{L^3}\right]^{1/2}. \tag{8}$$

Figure 2 shows how the error in V_g depends on the leg length L and the error in the 1-sec terrain height estimate. For example, if the terrain error is ±4 m, 70 km legs are needed to achieve $a \pm 1$ m s^{-1} rms error in V_g. If the terrain can be determined to ±1 m, the leg lengths could be reduced to 50 km for the same accuracy in V_g.

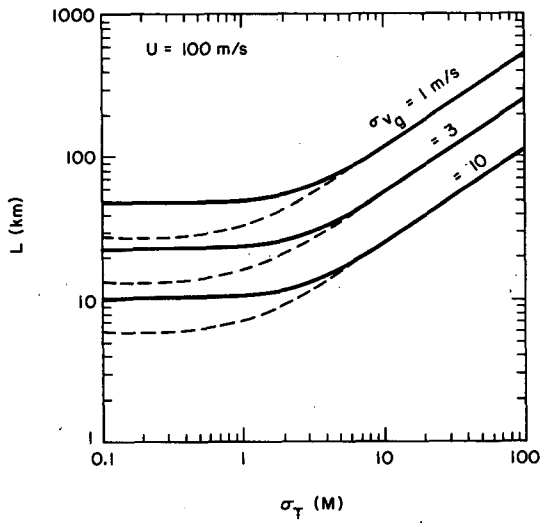

FIG. 2. Dependence of the error in geostrophic wind, σ_{V_g}, on the leg length, L, and error in terrain height estimate, σ_T. Solid line is for error in static pressure measurement of ±0.25 mb; dashed line ±0.1 mb.

a. Radar altimeter evaluation

A number of flight tests were performed to test the ability of the APN-159 to track terrain changes. It can easily be shown that even radar altimeter height errors of a few percent can lead to large errors in isobaric slopes over irregular terrain. This is especially true over the Great Plains because of the comparable magnitude of the terrain slope and the typical isobaric surface. Furthermore, for southerly geostrophic winds the isobaric slopes dip toward the west, opposite to the terrain gradient. Assuming a uniform terrain slope of 10^{-3}, and a perfect knowledge of the terrain, a 5% calibration error in the calculation of radar altitude causes height-related biases that would result in 60% error in the determination of a 10 m s^{-1} geostrophic wind (Fig. 1). Therefore, it is imperative that the radar altimeter scale factor be known to a high degree of precision.

Similar errors can occur when a time lag is present between the static pressure and the radar altimeter measurements. This time discrepancy prevents correct signal matching of terrain with radar altitude since corrections cannot be properly made for the variation of the aircraft from the reference pressure. Such errors are exaggerated as the terrain becomes more irregular, or when the aircraft deviates rapidly from the constant pressure surface. To minimize this problem, these test maneuvers were processed using the INS vertical accelerometer in the geometric altitude calculation, using the static pressure to damp errors in the accelerometer over periods >200 sec. The third-order inertial barometer loop used is similar to that reported by Blanchard (1971).

As part of the Great Plains LLJ field experiment in July 1983, three types of aircraft maneuvers were executed to test the reliability of the instrumentation in detecting isobaric slopes. To eliminate the influences of irregular terrain in these tests, the maneuvers were performed over Lake Ponca, a narrow, L-shaped body of water with straight segments of 5 and 3 km in length, located about 5 km east of the Ponca City, Oklahoma airport which served as the operations base for the experiment. To minimize the local land–water heating contrast, flights were conducted during the morning hours. The low-level winds were light (<5 m s^{-1}) throughout the test flight and the lake was undisturbed. The three maneuvers consisted of porpoising, rolling, and climbing motions. Porpoising was conducted to check the accuracy of the radar heights compared with the hydrostatically determined height, to verify that corrections can be made for the aircraft deviating from the selected pressure level, and to make sure that no time lag is present between static pressure and radar height measurements. The vertical profile provided a check on the radar altimeter scale factor with height computed from integrating the hydrostatic equation.

Rolling motions tested the tracking ability of the altimeter, in particular the ability to detect the leading edge of the returned pulse, essential to discerning the height of the surface directly under the aircraft.

Figure 3 shows the results of the porpoising maneuvers. The curves on the left side of the figure are the actual radar altitude traces. In most cases the individual vertical displacements varied from 50 to 100 m in about 10–15 sec and the entire maneuver covered the 5 km length of Lake Ponca. In several of the tests, a well-defined upward trend was present with the porpoising motions superimposed. The curves on the right-hand side of Fig. 3 represent the corresponding heights corrected to a fixed isobaric level. Height corrections were computed by integrating the hydrostatic relationship in which the mean temperature of the column of air was taken to be the linear average of temperature at the reference level and the temperature at the actual height. As can be seen in Fig. 3, deviations from the reference pressure level can be corrected with a high degree of precision. Root-mean-square (rms) errors from the reference level after correction were between 1 and 2 m for each porpoising maneuver. Small scale errors (±3 m) were in general random and were attributed to problems with the static pressure. A slight systematic bias was discovered in the porpoising data which is thought to be the result of backlash in the synchro gears. This bias is apparent when plotted on a finer scale as shown in Fig. 4. For each maneuver the general upward trend in the altimeter heights is completely corrected even though the short-term bias persists. This bias is shown to be ±3 m which is a serious noise factor for flights over highly irregular terrain. However, in the Great Plains LLJ experiment, terrain variations were much smaller than simulated in the porpoising maneuvers, and the errors would be smaller than this estimate.

The second series of tests were performed to ensure that the radar altimeter scale factor was correct. As before, the tests were conducted over Lake Ponca to eliminate uncertainties in the terrain. Soundings were conducted to a height of 1200 m over the lake. Comparisons of the radar height to the height computed from integrating the hydrostatic equation were made. The results are illustrated in Fig. 5 with the radar height, isobaric height, and difference shown. No long-term bias in the altimeter is evident. For a 5% long-term bias, a height error of 30 m over a 600 m sounding would result, and the right-hand curves in Fig. 5 would show a uniform slope. Absolute errors between the derived height and radar height were within 5 m. Most of the error again is thought to be in the static pressure measurement. From this test, it is concluded that the radar altimeter calibration is within about 1%. Again, the sounding shown is a severe test compared with the level altitude flown in the actual data legs.

The final series of tests consisted of rolling maneuvers to test the tracking ability of the altimeter. In particular,

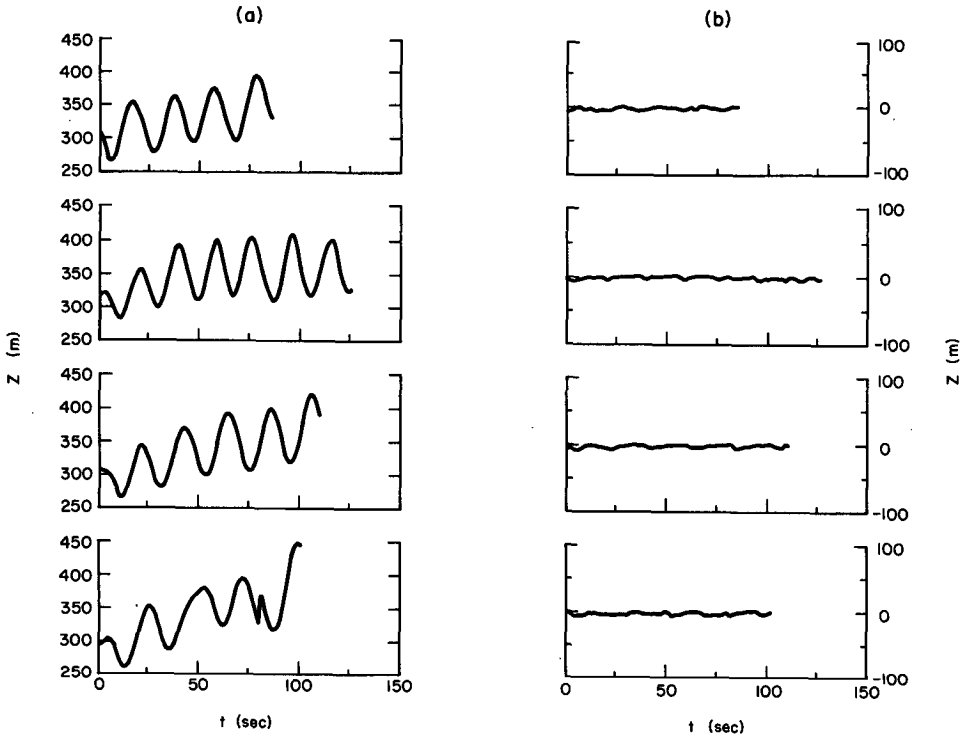

FIG. 3. (a) Radar altitude traces for porpoising maneuvers, and (b) altitude of isobaric surface above mean sea level after corrections have been applied for deviations of aircraft from isobaric surface.

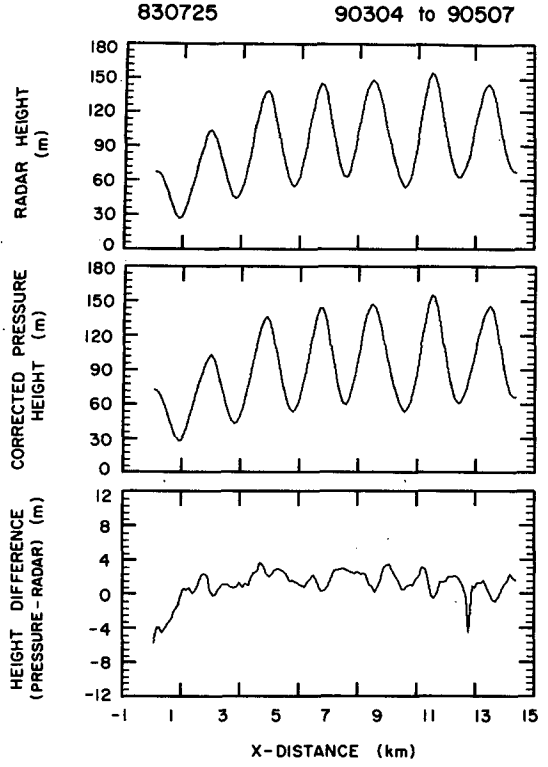

FIG. 4. Radar and pressure heights for porpoising maneuvers as in Fig. 3, except scale for difference is expanded to reveal residual error in isobaric height (lower panel).

the ability of the radar altimeter to detect the leading edge of the return pulse is of fundamental importance. Again, the maneuvers were performed over Lake Ponca. Maneuvers consisted of alternating rolls of up to 40° to the left and right. Examples of the tests are illustrated in Fig. 6 where it is evident that some bias exists during rolling motions. However, during the actual data legs care is taken to avoid such maneuvering.

b. Test of terrain registration

An analysis was performed to determine the sensitivity to errors in aircraft position of the geostrophic wind calculation. Even small errors in position over irregular terrain features may yield large errors in isobaric height determination. In the case of mesoscale application where the slope is quite small, accurate position becomes the crucial element in the analysis. INS drift errors of up to 1–2 km h^{-1} were expected to be unacceptable, but the accuracy requirement was not known prior to the field experiment. Flight legs on the Great Plains LLJ project were purposefully chosen along straight highways at low levels so that adequate visual checks were possible. Figure 7 shows the location of the field project area and the flight strategy. The precisely defined L-shaped flight paths were set along north–south (U.S. Highway 77) and east–west (state Highway 51) directions.

An example of an isobaric slope analysis from an east–west leg is shown in Fig. 8. Note that the top and middle panels are images of each other with the bottom panel being the difference. The top panel represents the measured aircraft radar altitude of the isobaric surface corrected for small deviations from constant pressure by integration of the hydrostatic equation. The middle panel shows the underlying terrain heights at each second along the aircraft path, obtained from USGS 1:24 000 topographic maps digitized on a 0.4 × 0.4 km grid. The lower panel is the resulting height of the isobaric surface above sea level, which is obtained by adding these two traces. (Note that the top two panels are nearly mirror images.) The straight line through the data in the lower panel was obtained from least-squares fit to the model of Eq. (1). Repeated passes are very similar except for changes in isobaric slope and any deviations from the usual track. From the least-squares calculation, estimates of the error in the slope as well as the residual variance of deviation from the fit are obtained. From the slope, the geostrophic wind can be computed with the geostrophic wind relationship of (2) using $\partial Z/\partial x$ as the isobaric slope.

To examine the sensitivity of this analysis to aircraft position error, the calculation was repeated for a range of x (east–west) and y (north–south) position errors at

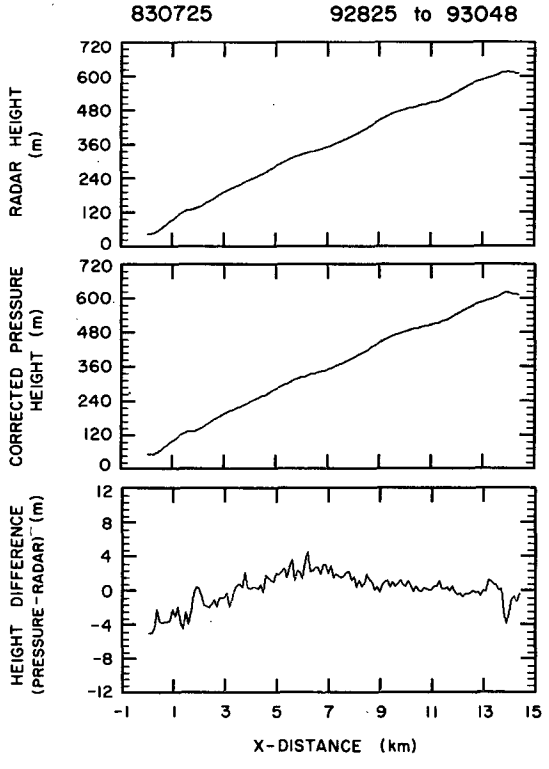

FIG. 5. Examples of radar altitude and corrected pressure altitude traces during sounding maneuver.

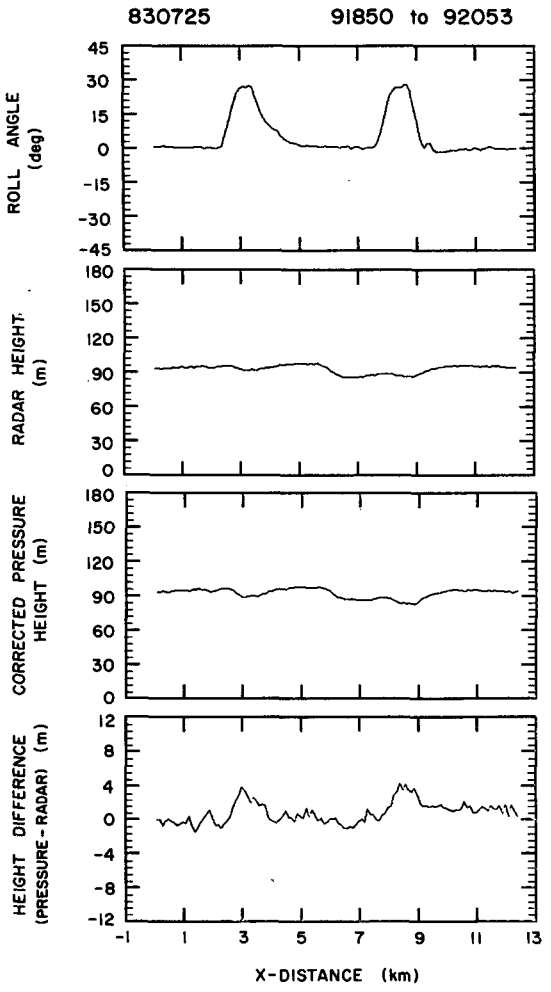

FIG. 6. Radar altitude and corrected pressure altitude traces during roll maneuvers.

0.1 km intervals from the nominal value obtained from integrating the INS velocities. During the 15–20 min legs, it is assumed that the INS position error is constant, and that deviations in x and y were well represented by the INS accelerometer. It is further assumed that a simple x or y translation of the data is all that is required for registration. In Fig. 9, the residual variance from the fit is plotted for each value of the possible x and y position errors for both the north–south and east–west legs. On the north–south leg, the residual variance from the isobaric surface was determined to be minimized to a value of about 2.5 m by adding a correction of -1.2 km in the y direction. On the east–west leg, which in this example was not flown close in time to the north–south leg, the deviations were minimized to a value of 3.6 m with a correction of 0.8 km in the x direction and 0.2 km in the y direction. The terrain in both directions appears to produce a single minimum at all reasonable values of the INS position error, so the process is analogous to "jiggling" a key in a lock until it fits, and the location of the minimum variance from the isobaric surface is considered to be the correct location.

In Fig. 10, the computed values of the geostrophic wind computed from the isobaric slope on the same legs are shown plotted as a function of different x and y position corrections. On the north–south leg, the derived isobaric slopes are relatively insensitive to x-position error, but a 1 km y-position error changes the value of the geostrophic wind by as much as 10 m s^{-1}. On the east–west leg, both x and y errors are equally important and similar geostrophic wind sensitivity is evident.

Estimates of the standard deviation in the estimate of the isobaric slope were made, and assuming that the errors are normally distributed, 95% confidence limits calculated, which are plotted in Fig. 11 as a function of x and y errors. On the north–south leg, the error minimizes at about 0.5 m s^{-1}. On the east–west leg, the error minimizes at about 1 m s^{-1}. Of course, terrain biases are not randomly distributed along the track so that these errors are underestimates of the true error. Nonetheless, these calculations suggest that to obtain 1 m s^{-1} accuracy in the geostrophic wind determination, aircraft position must be known to <250 m.

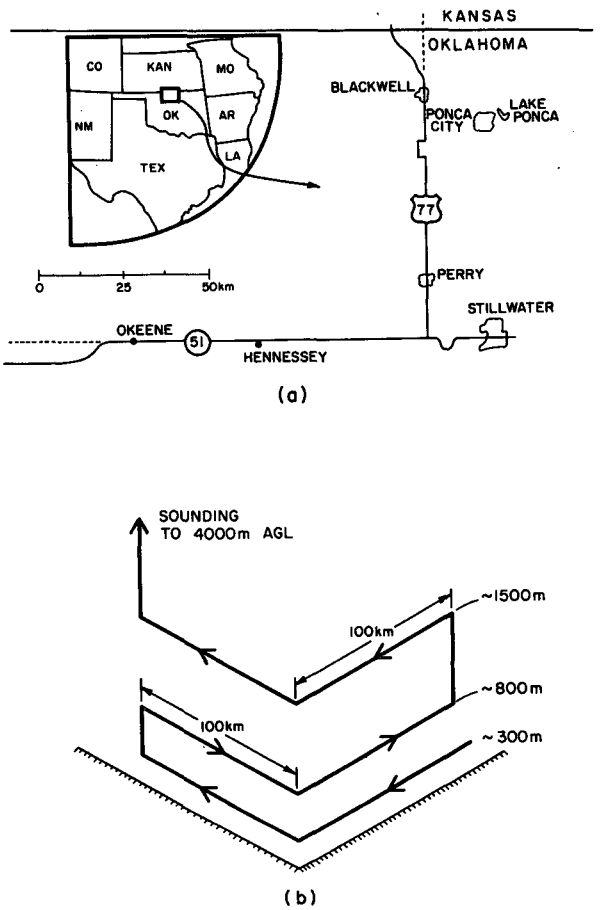

FIG. 7. Map of (a) field site, and (b) flight profiles.

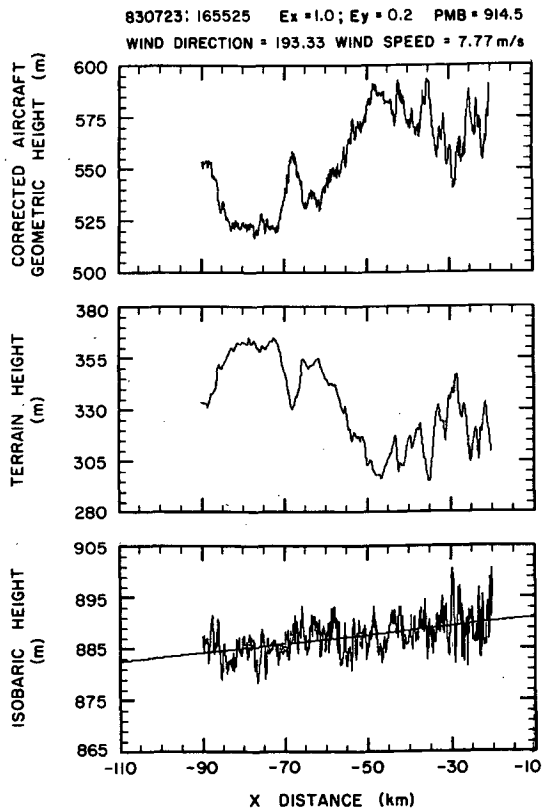

FIG. 8. Isobaric slope analysis for east–west leg on 23 July 1983 at 914.5 mb level beginning at 1655 LST. (Top) Radar altitude corrected for small deviations of the aircraft form the constant pressure surface; (middle) terrain height from digitized 1:24 000 scale topographic maps at location of aircraft; (bottom) isobaric height resulting from sum of radar altitude and terrain height. Straight line through bottom panel is least-squares fit to isobaric heights. Aircraft position has been adjusted to minimize variance from a straight line resulting in corrections E_x and E_y (km) indicated.

4. Examples of horizontal pressure gradients and geostrophic winds on 100 km scale

In this section, we present some examples of the measurements obtained using the techniques described in this paper. A complete description of the Great Plains LLJ is reported by Parish et al.

Repeated passes at constant pressure down the east–west road should result in radar altimeter traces that are the same allowing for minor deviations from the desired track and any change in the height of the constant pressure surface. In Fig. 12, traces of Z_P indicate a downward trend in the altitude from pass to pass. In Fig. 13 for this same case, the average height of the pressure surface for eight passes is plotted versus time revealing a small but steady fall of the pressure surface on the order of 0.2 cm s^{-1}. Over the time it takes to fly one leg (20 min), this pressure tendency results in a fall of about 4 m from the beginning of the run to the end of the run which, if not accounted for, would appear to be a V_g of about 4 m s^{-1} using Eq. (2) for the 100 km leg. On the reciprocal leg, this effect would repeat, but with the opposite sense so that on repeated runs there would appear to be an oscillating V_g of about 4 m s^{-1} added to the actual value of V_g. It is imperative, therefore, to remove this pressure tendency from the data prior to performing the pressure gradient analysis. Averaging legs flown in opposite directions would compensate for this if the pressure were varying linearly with time, but this decreases the ability to resolve short-term (~20 min) changes.

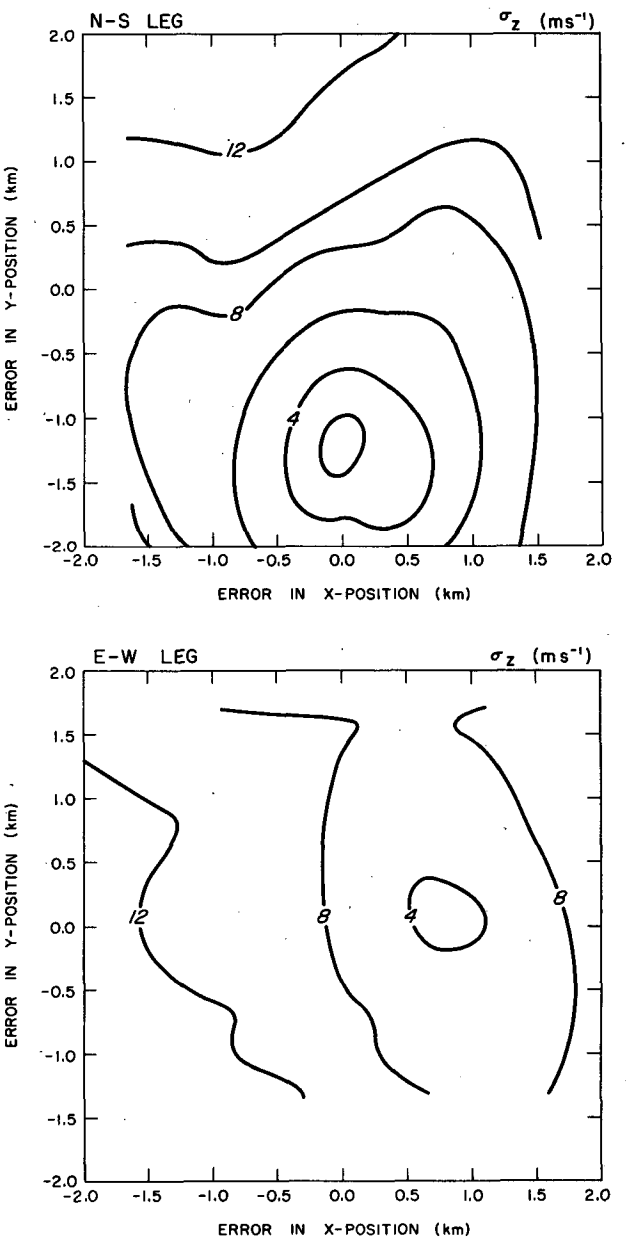

FIG. 9. Residual variance from least-squares fit to isobaric height data as a function of error in x and y positions for north–south and east–west legs.

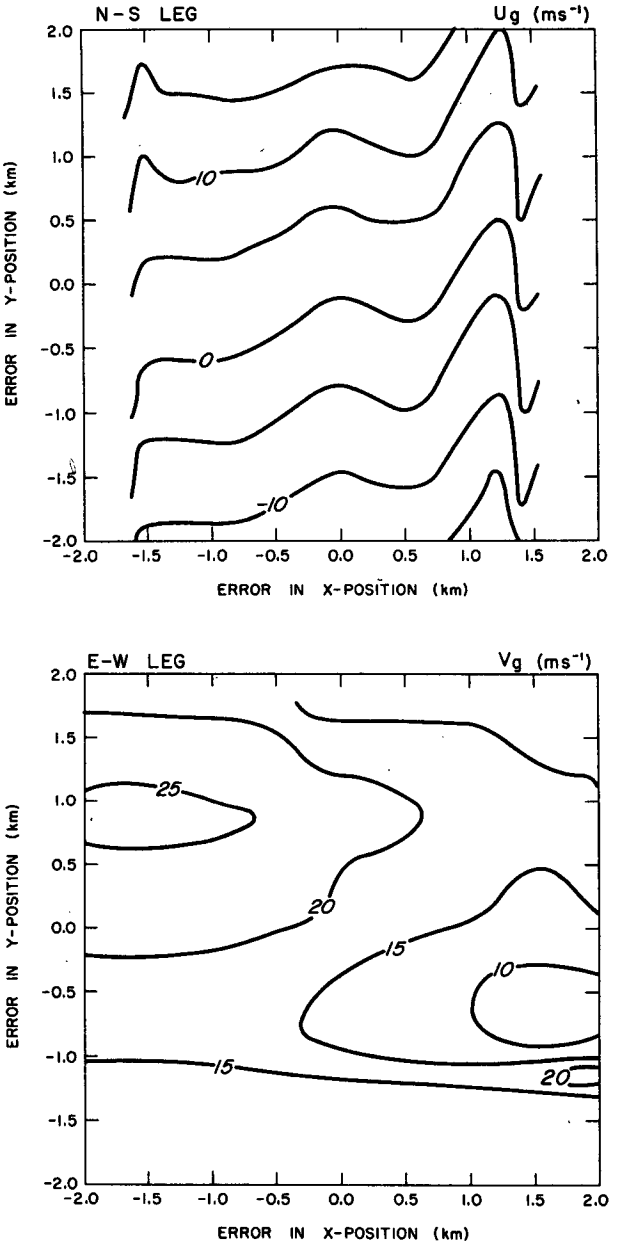

FIG. 10. Geostrophic wind components computed from isobaric slopes for north–south (U_g) and east–west (V_g) legs as a function of error in x and y position.

Because the largest pressure gradients are nearest to the surface, the pressure tendencies at each level may not be the same. In Fig. 14, we show the results of an analysis of the 23 July 1983 case discussed by Parish et al. where the pressure tendency is not constant with time nor altitude. Particular care must be given to these effects in order that V_g estimates good to 1 m s^{-1} can be achieved.

In Fig. 15, V_g is plotted over a 2-h period centered at about 1400 LST when the changes in the pressure gradient are small but steady. We show here that the techniques described produce consistent estimates of the pressure gradients and V_g, after all the corrections are applied with an error estimated to be less than about 1 m s^{-1}.

5. Conclusions

Measurement of the horizontal pressure gradient force is fundamental to the understanding of the evolution of the windfield. However, isobaric slopes are

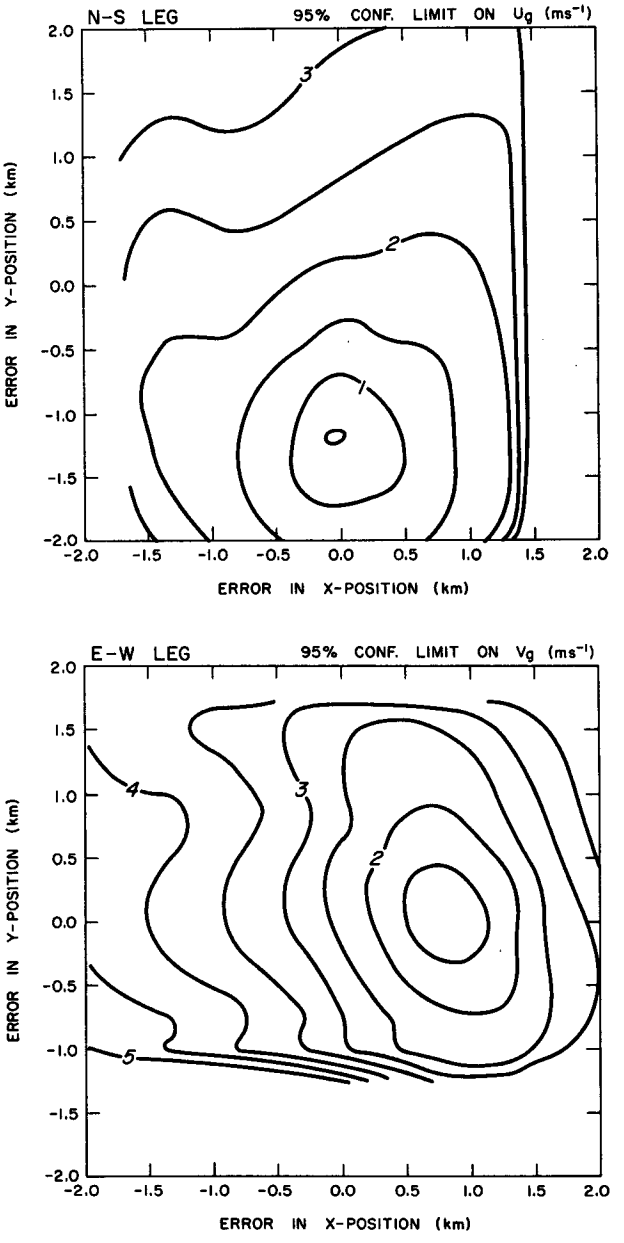

FIG. 11. Estimates of 95% confidence limits on geostrophic wind components on north–south and east–west legs as a function of error in x and y position.

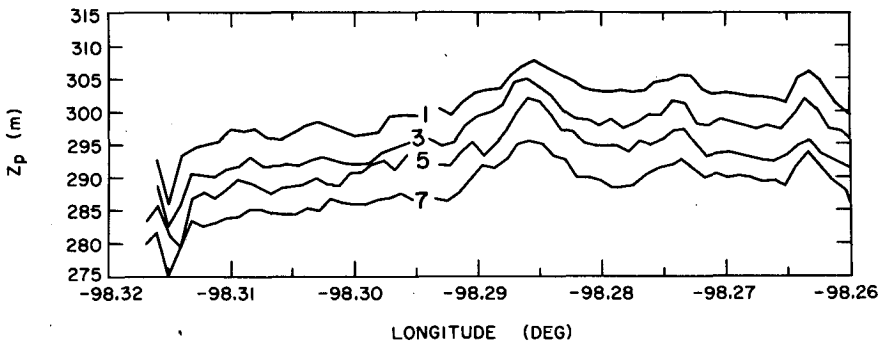

FIG. 12. Height of the constant pressure surface above ground level (after correction for aircraft deviations) as a function of longitude for east–west legs flown on 28 March 1986. Numbers 1, 3, 5, 7 indicate order of repeated legs.

very small and measurement is difficult when the horizontal scale is small. The inherent small errors in radiosonde sensors generally limit their usefulness in geostrophic wind calculations. Furthermore, the relatively large space and time scales of the upper air observations severely limit potential mesoscale application. An alternate approach in isobaric slope determination is airborne radar altimetry. The purpose of this paper has been to evaluate the errors associated with measurement of mesoscale pressure gradients on distances <100 km over complex terrain, and to demonstrate the usefulness of these measurements in studies of the Great Plains LLJ. While in principle this concept is simple, even small errors in instrumentation can produce significant errors in V_g. It is therefore imperative that the onboard instrumentation be thoroughly tested. It has been shown that a variety of maneuvers are useful in ensuring that the altimeter measurements are reliable. From tests conducted as part of the Great Plains LLJ field experiment, it is concluded that the altimeter measurements are calibrated to within 1% and that hydrostatic corrections for minor excursions off the isobaric surface by the aircraft are very accurate. It also has been shown that proper registration between the aircraft altimeter data and the terrain data is crucial, and that <0.25 km positioning accuracy is needed to produce geostrophic wind estimates within 1 m s^{-1}. Uncertainties about the profile of underlying terrain ultimately limit the analysis, but the present errors in the determination of geostrophic winds on the 100 km scale are ± 1 m s^{-1} over the rolling terrain of the Great Plains. We feel that similar accuracies can be achieved over other terrain types provided that accurate terrain data can be obtained. LeMone and Tarleton (1986)

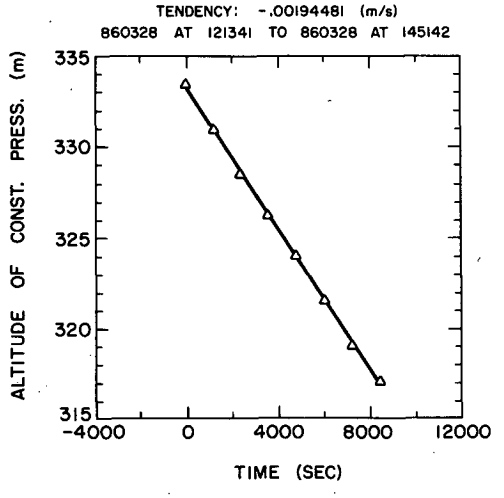

FIG. 13. Altitude of constant pressure surface (Z) for east–west and north–south passes made over a period of 2.5 hours. Altitude has been normalized to a single pressure level using hydrostatic corrections based upon actual measured temperature structure. Solid line represents tendency of pressure of -0.002 m s^{-1} over this period.

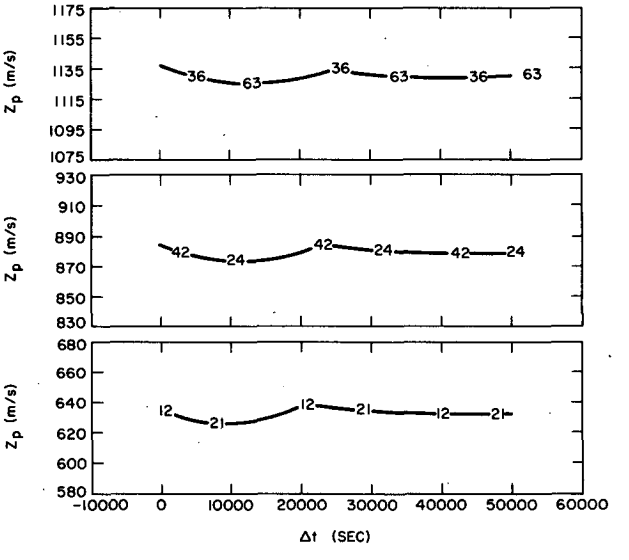

FIG. 14. Altitude of constant pressure surface (Z) for east–west and north–south passes made over a 14-h period on 23 July 1983: 890 mb (top), 915 mb (middle) and 940 mb (bottom). Sequential pass numbers are indicated.

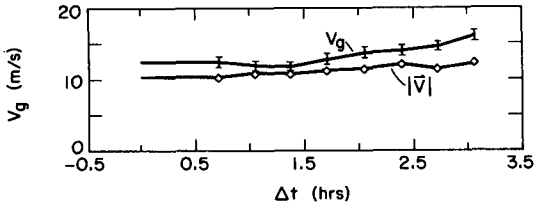

FIG. 15. Evolution of V_g on 28 March 1986 from isobaric slopes measured on east–west passes. Error bars are the result of the least-squares fit. Actual wind magnitudes are indicated (◇).

point out that combining the inertial altitude technique for short wavelengths with the radar altimetry technique for longer wavelengths would provide pressure fields on scales even shorter than 100 km but greater than cloud scale.

In addition to accurate estimates of geostrophic wind components, we feel that research aircraft instrumented as described here can provide very precise estimates of vertical wind $\omega = dp/dt$ derived from the pressure tendency and advection terms that result from this analysis (e.g., Fig. 12). A wide range of applications of the isobaric slope measurement technique on the mesoscale is envisioned.

Acknowledgments. Collection of data for this project involved long and fatiguing hours in the aircraft. Special thanks are extended to the flight crews consisting of Mr. Bill Zinser, Dr. Wayne Sand, Mr. George Bershinsky, Mr. Larry Irving, Mr. Robert Hanson, and Mr. John White. Flight operations were arranged and supported by the NCAR Research Aviation Facility. We would also like to thank the crew at the NOAA Boulder Atmospheric Observatory for the data and for their logistical help with the tower flyby. This research was supported by National Science Foundation Grants ATM-8303191 and ATM-8502517.

REFERENCES

Bellamy, J. C., 1945: The use of pressure altitude and altimeter corrections in meteorology. *J. Meteor.*, **2,** 1–79.

Bevington, P. R., 1969: *Data Reduction and Error Analysis for the Physical Sciences,* McGraw-Hill, 336 pp.

Blanchard, R. L., 1971: A new algorithm for computing inertial altitude and vertical velocity. *IEEE Trans. Aerospace and Electronic Sys.,* **AES6,** 1143–1146.

Brown, E. N., M. A. Shapiro, P. J. Kennedy and C. A. Friehe, 1981: The application of airborne radar altimetry to the measurement of height and slope of isobaric surfaces. *J. Appl. Meteor.,* **20,** 1070–1075.

Cooper, W. A., 1978: Cloud physics investigations by the University of Wyoming in HIPLEX 1977. Dept. of Atmospheric Science, University of Wyoming, 320 pp.

Holton, J. R., 1979: *An Introduction to Dynamic Meteorology,* Academic Press, 391 pp.

Knowlton, D., 1980: Static pressure measurements. *Newsletter on Developments of Airborne Cloud Physics Instruments,* NCAR, **12.**

LeMone, M. A., and L. F. Tarleton, 1986: The use of inertial altitude in the determination of the convective-scale pressure field over land. *J. Atmos. Oceanic Technol.,* **4,** 650–661.

Parish, T. R., A. R. Rodi and R. D. Clark, 1987: A case study of the summertime Great Plains low-level jet. *Mon. Wea. Rev.,* in press.

Shapiro, M. A., 1970: On the applicability of the geostrophic approximation to upper-level frontal-scale motions. *J. Atmos. Sci.,* **27,** 408–420.

——, and P. J. Kennedy, 1981: Research aircraft measurements of jet stream geostrophic and ageostrophic winds. *J. Atmos. Sci.,* **38,** 2642–2652.

——, and ——, 1982: Airborne radar altimeter measurements of geostrophic and ageostrophic winds over irregular topography. *J. Appl. Meteor.,* **21,** 1739–1746.

Uccellini, L. W., and D. R. Johnson, 1979: The coupling of upper- and lower-tropospheric jet streaks and implications for the development of severe convective storms. *Mon. Wea. Rev.,* **107,** 682–703.

——, P. J. Kocin, R. A. Petersen, C. H. Wash and K. F. Brill, 1984: The Presidents' Day cyclone of 18–19 February 1979: Synoptic overview and analysis of the subtropical jet streak influencing the precyclogenetic period. *Mon. Wea. Rev.,* **112,** 31–55.